

2. Atmospheric and Oceanic Environment Modeling

Study of Basin-Scale Ocean Circulation related to Global Chlorophyll Distribution – Interdecadal Variation –

Contact Person

Laboratory head, Masahiro Endoh
Meteorological Research Institute,
Tsukuba, 305 Japan

(Research Organization)

Atsushi Obata, Yoshiteru Kitamura, Goro Yamanaka, and Tatsuo Motoi
Meteorological Research Institute

Keywords

global ocean circulation model, surface mixed layer, chlorophyll, climate change

1. Background

Recently, effects of human activity are expanding to the global ocean scale. Necessity of evaluating anthropogenic effects is increasing. As a first step towards this purpose, it is necessary to evaluate natural variations of oceanic environment distinguished from variations caused by human activity. Surface chlorophyll concentration as oceanic primary productivity is an important indicator of oceanic nutrient distributions related to the environmental deterioration, and is also an important element of global carbon cycle in concerning global warming. In the previous studies by use of ocean circulation models, hydrographic data, and satellite ocean color data, we globally discussed that the annual surface chlorophyll distribution depends on the upwelling distribution in the surface layer (Endoh et al., 1994a) and that the seasonal variation of chlorophyll is well explained by the seasonal variation of surface mixed-layer depth (Endoh et al., 1995; Obata et al., 1996). Based on these studies, climate change of oceanic environment is now an important subject to be studied, and the study will contribute to future analyses of anthropogenic effects.

2. Objective

Recent climate change has been studied by the analyses of physical and biogeochemical oceanic environments. Venrick et al. (1987) reported that the primary production of the central North Pacific increased in the mid 1970s and the time series are divided into two periods such as the late 1960s to the early 1970s (the low chlorophyll years) and the late 1970s to the early 1980s (the high chlorophyll years). They suggested that intensified westerly winds corresponding to intensification of the north-south gradients of sea level pressure in the mid 1970s enhanced upward transport of nutrients from depths by intensified vertical mixing, and the primary production increased in the euphotic and oligotrophic North Pacific subtropical gyre region. Polovina et al. (1995) verified the decadal and basin-scale variation in the mixed-layer depth and its impact on biological production in the central North Pacific by use of 1960-1988 hydrographic data and a plankton model. Using these studies as references, future studies of climate changes require self-consistent models which determine the physical, chemical, and biological values by their own dynamics, such as an ocean circulation

model with biogeochemical processes. As a first step, in the present study, we focus on the climate change of physical environments such as sea surface temperature, upwelling, and mixed-layer depth from 1960s to 1980s by use of the global ocean circulation model (Endoh et al., 1994a, 1994b, 1995).

3. Method

A numerical model employed is a standard global ocean circulation model with realistic bottom and coastal topography and resolution of $2.5^\circ \times 2^\circ \times 21$ levels (Endoh et al., 1994a). Embedded in the model is a turbulent mixed layer model which has a closure scheme of level 2 (Mellor and Yamada, 1982) with 5 meters resolution in the upper 20 meters. In the previous study (Endoh et al., 1994b), the model was driven by the monthly climatological wind stress (Hellerman and Rosenstein, 1983), monthly sea surface temperature and seasonal sea surface salinity (Levitus, 1982) after equilibrium calculation with the annual mean climatological forcing (Endoh et al., 1994a). The calculation was carried out for 11 years until it reaches to a quasi-steady state with seasonal variation.

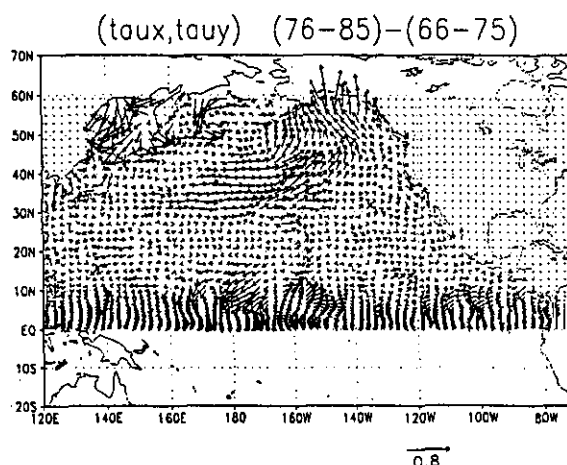


Figure 1. Difference of wind stress between 1976-1985 and 1966-1975 derived from the North Pacific wind stress data (Japan Meteorological Agency, 1994). The unit is dyne cm^{-2} .

Starting from this state, the North Pacific of the model is subsequently driven for 30 years by the 1961-1990 monthly wind stress and 1961-1990 monthly sea surface temperature (Japan Meteorological Agency,

1994) in order to evaluate the climate variation of oceanic physical environment in that region (Venrick et al., 1987; Polovina et al., 1995). Figure 1 shows the difference between 1976-1985 and 1966-1975 of the wind stress for the typical increase of westerlies over the central North Pacific. The seasonal climatological surface salinity (Levitus, 1982) is used as the haline forcing in the North Pacific because we have sparse historical salinity data for climate variation. Other oceanic regions of the model are driven by the climatological forcing (Endoh et al., 1994b).

4. Results

In order to be consistent with Venrick et al. (1987) and Polovina et al. (1995), we analyze the model results by comparing the averaged fields of the period of 1976-1985 with those of 1966-1975.

The difference of model sea surface temperatures (top 5 m average) between 1976-1985 and 1966-1975 is shown in Figure 2. SST is lower in the period of 1976-1985 than 1966-1975 in the central North Pacific. The anomaly reaches -0.6°C in the middle latitudes around the date line. These features are direct reflections of the interannual variations of the surface boundary conditions (JMA, 1994), especially SST data of 1961-1990. The difference of temperature fields above 1000 m between 1976-1985 and 1966-1975 is also shown along the date line (180°E) in Figure 3. Water temperature in the intermediate layer is higher in 1976-1985 than 1966-1975 in the lower latitudes of the North Pacific, and is lower in the higher latitudes. The intensified westerly winds of 1976-1985 around the middle latitudes of the central North Pacific (Figure 1) enhance the downward Ekman pumping in the lower latitudes and the Ekman upwelling in the higher latitudes (Figure 4), which leads to the temperature anomaly shown in Figure 3.

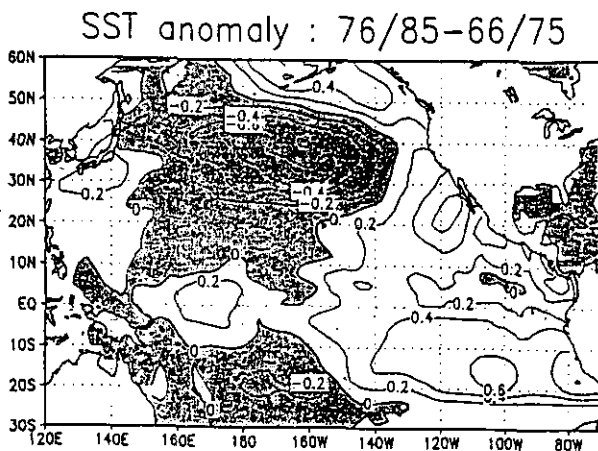


Figure 2. Difference of sea surface temperatures (top 5 m average) between 1976-1985 and 1966-1975 in the model forced with climate change of the North Pacific (JMA, 1994). The unit is $^{\circ}\text{C}$. Shaded areas denote regions where SST of 1976-1985 is lower than 1966-1975.

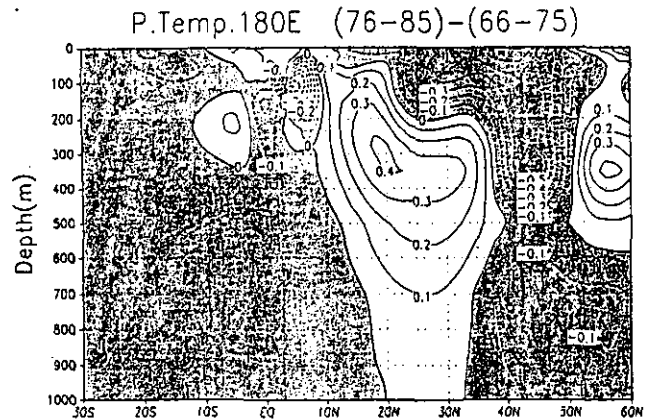


Figure 3. Difference of water temperature above 1000 m between 1976-1985 and 1966-1975 along the date line in the model. The unit is $^{\circ}\text{C}$. Shaded areas denote regions where temperature of 1976-1985 is lower than 1966-1975.

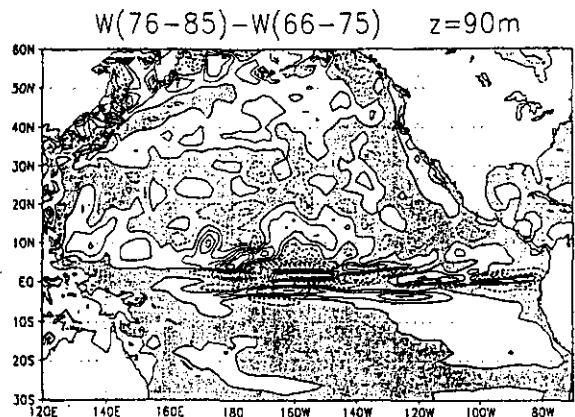


Figure 4. Difference of vertical velocity at the depth of 90 m between 1976-1985 and 1966-1975 in the model. The contour interval is $4 \times 10^{-7} \text{ m s}^{-1}$. Shaded areas denote regions where the tendency of downwelling is stronger in 1976-1985 compared with 1966-1975.

The difference of the surface mixed-layer depth (MLD) between 1976-1985 and 1966-1975 is shown in Figure 5. MLD is defined as the depth where the downward temperature deviation in a vertical grid column reaches 0.5°C measured from the sea surface (Endoh et al., 1994b, 1995; Obata et al., 1996). MLD is deeper in 1976-1985 than 1966-1975 in the lower and middle latitudes of the central North Pacific, while MLD is shallower in the subarctic regions. These patterns of the model are consistent with the hydrographic analysis of Polovina et al. (1995). Figure 6 shows the interannual variation of MLD at the grid point of the central North Pacific (28°N , 155°W) which is in the same region as that studied by Venrick et al. (1987). Deeper mixed layers are found in the winter season of 1980, 1983, and 1986. It is expected that

these intensified vertical mixings cause the increase of primary production in the low latitudes by increased upward nutrient transports. This model result is consistent with Venrick et al. (1987).

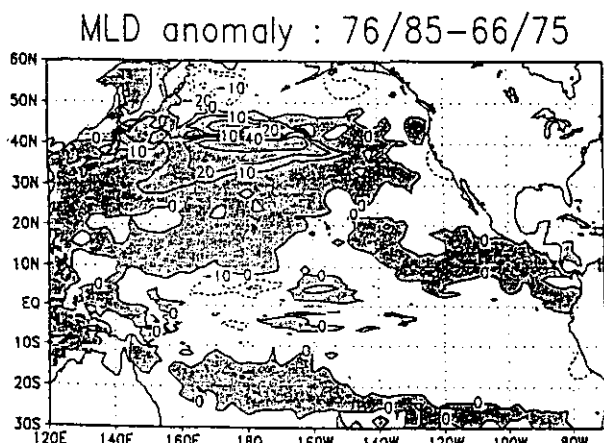


Figure 5. Difference of surface mixed-layer depth (MLD) between 1976-1985 and 1966-1975 in the model. The unit is meter. Shaded areas denote regions where MLD of 1976-1985 is deeper than 1966-1975.

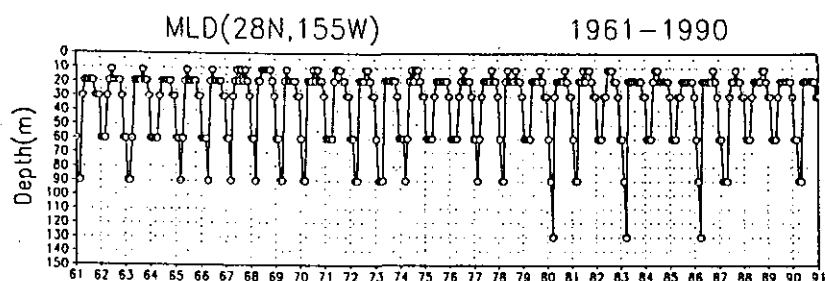


Figure 6. Interannual variation of mixed-layer depth at the grid point of the central North Pacific (28°N, 155°W) from 1961 to 1990 in the model.

5. Summary

Interannual variations of North Pacific physical environments in a global ocean circulation model (with a turbulent closure mixed layer model) with forcing of the North Pacific climate changes (JMA, 1994) are compared with physical and biological climate changes reported in the previous studies (Venrick et al., 1987; Polovina et al., 1995). Deepening of mixed layer from the period of 1966-1975 to 1976-1985 is found in the central North Pacific of the model, which is consistent with the previous studies in terms of physical environments.

In future study, biogeochemical processes will be embedded in the ocean circulation model in order to examine interaction between the climate changes and the global elemental cycles.

References

- Endoh, M., et al., *CGER's Supercomputer Activity Report 1992*, 31, 1994a.
- Endoh, M., et al., *CGER's Supercomputer Activity Report 1993*, 23, 1994b.
- Endoh, M., et al., *CGER's Supercomputer Activity Report 1994*, 21, 1995.
- Hellerman, S., and M. Rosenstein, *J. Phys. Oceanogr.*, 13, 1093, 1983.
- Japan Meteorological Agency, *Ocean Surface Fluxes in the North Pacific*, 1994.
- Levitus, S., *NOAA Prof. Pap.* 13, 173pp., 1982.
- Mellor, G. L., and T. Yamada, *Rev. Geophys. Space Phys.*, 20, 851, 1982.
- Obata, A., J. Ishizaka, and M. Endoh, *J. Geophys. Res.*, 101, 1996. (in printing)
- Polovina, J. J., G. T. Mitchum, and G. T. Evans, *Deep-Sea Res.*, 42, 1701, 1995.
- Venrick, E. L., J. A. McGowan, D. R. Cayan, and T. L. Hayward, *Science*, 238, 70, 1987.

Development of the Transport, Transformation and Removal Model for Acidic and Oxidative Pollutants in the East Asia

Contact person

Junji Sato
Applied Meteorology Research Department, Meteorological Research Institute
Japan Meteorological Agency

(Research Organization).

Hidetaka Sasaki
Takehiko Satomura

Key words Numerical Model, Lagrangian particle, Nesting, Sulfur Oxides, Deposition

1. Background

More than 24 million tonnes/year of anthropogenic sulfur oxides is emitted into the atmosphere, and about 70% of this value is predominated by emission sources in Asian continent. Thus concern about acid deposition originated in continental emission sources has increased in the East Asian region.

2. Objective

It is very difficult to estimate the amounts of acid deposition in the East Asian region because of no monitoring network have been set up. One way to circumvent this difficulty is by using numerical models. It have been said that the in-cloud scavenging process plays important role in wet deposition¹⁾. In order to include the in-cloud scavenging process in the transport model(MRI-LTM), therefore, the MRI-LTM was improved to gain higher spatial resolution.

3. Outline of the Model

The MRI-LTM consists of two main submodels which combine by off-line system; a meteorological model which predicts meteorological variables, and dispersion model which includes processes of advection, diffusion, deposition and chemical transformation of SO_2 to SO_4^{2-} .

Two meteorological models are combined by nesting method to gain high spatial resolution over focused area. The spectral boundary coupling method²⁾ is used for the nesting. The calculation domain of the outer model is about $9300 \times 7000 \text{ km}^2$ divided by 73×55 grids with 127 km of the horizontal spatial resolution, and has 16 layers in the vertical. The inner model has a regular 97×97 square transform grid with a grid distance of about 40 km. The model also uses σ -coordinate system and has 19 layers in the vertical.

Advection and diffusion of sulfur oxides are described by a Lagrangian particle with random-walk model in the same coordinate system as in the meteorological submodel. A particle is assumed to be deposited by a dry and wet process. The only chemical transformation in this model is that of SO_2 to SO_4^{2-} .

4. Application to the East Asian Region

The simulation of transport process of sulfur oxides over the East Asian region was performed for whole year of 1985. The emission inventory of sulfur oxides for 1985's were redistributed to 80 point sources based on industrial activities and population of the major cities³⁾. The 80 point sources include emissions at Japan and Far East of Russia but for volcanic and other natural

emission sources. The distribution of dry and wet deposition for the period from 20th to 24th Jan. 1985 is shown in Fig. 1.

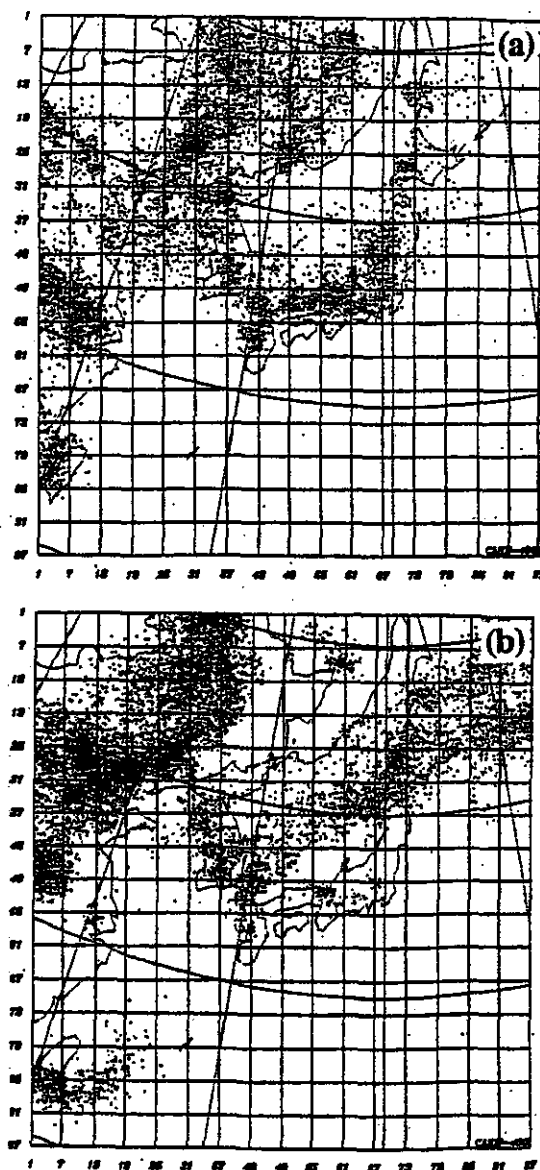


Fig. 1 Distribution of dry (a) and wet (b) deposition of SO_2 during the 5 days from 20th to 24th Jan. 1985.

In the case of wet deposition, the distribution does not shown systematic because it only depends on the area of precipitation. Therefore, the transport model requires to capture readily the precipitation. For this reason, we

have been lavished much care on the meteorological submodel in present study.

The distribution of dry and wet deposition for 5 days from 13rd to 17th August 1985 is also shown in Fig. 2. Contrary to prevail northwest wind in winter, southerly wind prevailed during summer, sulfur oxides are flown for the north direction around Japan because of weak southerly wind during the period. In consequence, wet deposition of sulfur oxides originated from emission sources in Japan occurred at the area from central part of the Sea of Japan to the Sea of Okhotsk as seen in Fig. 2.

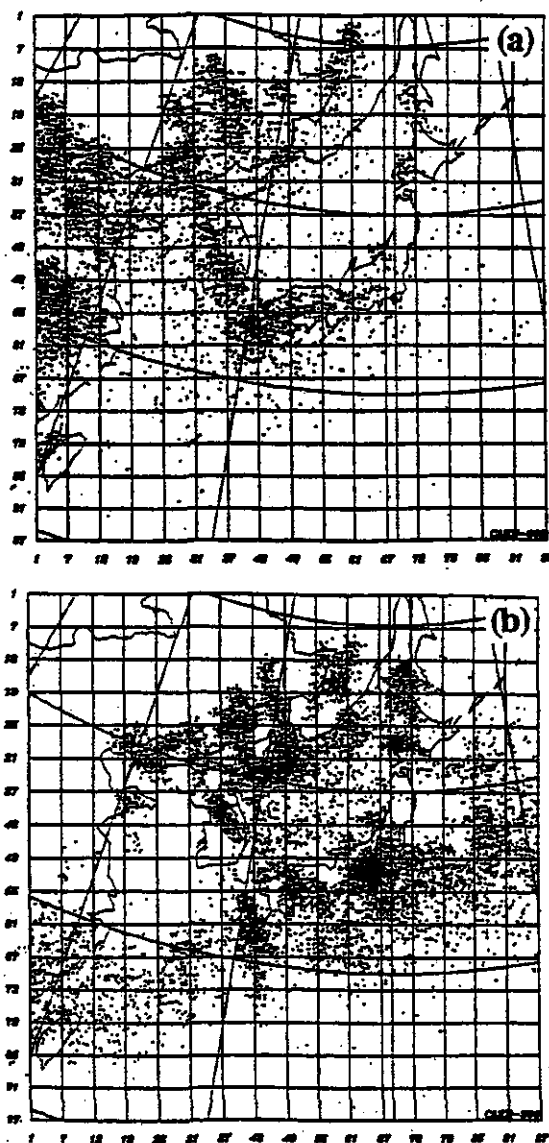


Fig. 2 Same as Fig. 1, but for the period from 13rd to 17th Aug. 1985.

5. Concluding remarks

In order to be skillful in the wet deposition process, the improvement of meteorological submodel was carried out. Owing to get higher spatial resolution while keeping wider model domain such as the East Asian region, the spectral boundary coupling method was used. After the validation of nested method, the availability of the MRI - LTM was also validated by the test simulation of radioactive pollutants emitted from Chernobyl.

The Application run of the MRI-LTM was performed for the transport and removal of sulfur oxides over the East Asian region. Simulation was carried out and adequate results were obtained. Since the Lagrangian particle method was used in present model, it was possible to determine the source-receptor relations. The model is avail to investigate the impact for deposition originating from the continental emission sources.

References

- 1) Flossmann, A., 1991: The scavenging of two different types of marine aerosol particles calculated using a two-dimensional detailed cloud model. *Tellus*, 42B, 463-480.
- 2) Sasaki, H., H. Kida, T. Koide and M. Chiba, 1995: The performance of long-term integration of a Limited Area Model with the spectral boundary coupling method. *J. Met. Soc. Japan*, 73, 165-181.
- 3) Sato, J., T. Satomura, H. Sasaki and Y. Muraji, 1995: The long-range transport model of sulfur oxides and its application to the East Asian region. *Technical Report of the Meteorological Research Institute*, No. 34, 1-101.

A Study of Modeling of Local CO₂ Circulations

Contact Person

Laboratory Head, Yasuo Sato
Applied Meteorology Research Department
Meteorological Research Institute
Japan Meteorological Agency, Ministry of Transport
1-1 Nagamine, Tsukuba-shi, Ibaraki 305, Japan
Tel: +81-298-53-8614 Fax: +81-298-55-7240
E-mail: ysato@mri-jma.go.jp

(Research Organization)

Kazuo Mabuchi, Masaru Chiba, Takashi Koide, Kiyotaka Shibata
Climate Research Dept., Meteorological Research Institute
Hidetaka Sasaki, Takehiko Satomura, Kazuyo Adachi, Akira Yamamoto
Applied Meteorology Research Department
Takehisa Oikawa, Nobuko Saigusa
Institute of Biological Sciences, University of Tsukuba

Key Words

Climate model, Biosphere model, CO₂ flux, C₃ plants, C₄ plants

1. Introduction

It is an especially important and basic issue to make clear the mechanism of carbon dioxide (CO₂) circulations and budgets in the study of global warming. The so-called "CO₂ missing sink issue" shows that we have not had sufficient knowledge of CO₂ circulations. Unless we can make clear the problem, it is difficult to draw the future image of the global warming phenomenon.

The CO₂ circulations are deeply influenced by ecosystems, and especially through local weather and climate. Thus, we need to simulate CO₂ circulations after modeling local weather and climate in a model study of CO₂ circulations.

In this study, we firstly construct the model of the relationship between local weather and surface hydrology processes including land ecosystems. Secondly, we numerically simulate daily variations of atmospheric CO₂ concentration by estimating CO₂ fluxes in the model. As a result, we can estimate the atmospheric CO₂ concentration. By doing so, it will be possible to evaluate the role of processes associated with so-called "CO₂ missing sink" and their relative degree of importance.

Vegetation plays an important role in the global energy, water, and carbon cycles through its evapotranspirative, photosynthetic and respiratory

activities. Recently, realistic biosphere models were presented by Dickinson¹⁾(1984) and Sellers et al.²⁾(1986) for use in GCMs. Several studies have been conducted to investigate the interactions between land surface processes and atmospheric phenomena using these models (Dickinson and Henderson - Sellers³⁾, 1988; Sato et al.⁴⁾, 1989).

The energy, water and CO₂ exchanges between vegetated surface and atmosphere have been studied by many researchers in the scale of plant canopy (e.g., Horie⁵⁾, 1981; Ohtaki⁶⁾, 1985; Baldocchi⁷⁾, 1994; Fan et al.⁸⁾, 1995). The energy and mass fluxes over natural vegetation are, however, not yet readily predictable. For example, grasslands in the mid-latitude consist of C₃ and C₄ plants, and the contribution of C₃ and C₄ plants to the above-ground biomass often changes with season and climatic conditions.

Generally, C₄ plants have a higher optimum temperature for photosynthesis and higher water use efficiency than C₃ plants, and the effects of atmospheric CO₂ concentration on the plant biomass and net primary production are different between C₃ and C₄ grassland (Oikawa⁹⁾, 1995). The geographic distribution and eco-physiological responses of C₃ and C₄ plants have been investigated in several grasslands in the world (

Hattersley¹⁰⁾, 1983; Cavagnaro¹¹⁾, 1988; Kalapos¹²⁾, 1991). However, the effects of the changes in the biomass of C₃ and C₄ plants on the energy and mass fluxes over the canopy have not been well understood. Long-term field measurements are thus required to obtain more information about energy and mass fluxes relating with spatial and temporal variations in plant species.

2. Research Method

Firstly, we develop a high-quality nested local climate model. Secondly, we develop a simple surface hydrology model including plant physiological processes for use in a 3-dimensional local climate model. In that model, we treat explicitly CO₂ fluxes between the atmosphere and land surface ecosystems according to daily variations of local weather. Thirdly, we will simulate the local CO₂ circulations and budgets with use of the developed model. Lastly, through analyzing results of the model simulations, we will investigate the role of variety of processes associated with the so-called "CO₂ missing sink", and their degree of relative importance.

On the other hand, the aim of the present study in University of Tsukuba is to measure CO₂ flux by the gradient method over a grassland containing C₃ and C₄ plants. The seasonal change in CO₂ flux measured by the gradient method was analyzed from the ecological and meteorological point of view over an artificial grassland containing C₃ and C₄ plants in University of Tsukuba. The three dominant species of the grassland belonged to the Gramineae; *Festuca elatior* (C₃) dominated in early spring, and *Imperata cylindrica* (C₄) and *Andropogon virginicus* (C₄) grew during early summer and became dominant in mid-summer. (Fig.3)

3. Results and Discussion

3.1 Development and Verification of a Biosphere-Atmosphere Interaction Model (BAIM) for use within physical climate models.

A Biosphere-Atmosphere Interaction Model (BAIM) for use within physical climate models was developed (Fig.1). BAIM has two vegetation layers and three soil layers, and the temperature of each layer and moisture stored for each layer are predicted. In the presence of snow on the ground, the snow layer is divided into a maximum of three layers, and the temperature and the amount of snow and water stored in each layer are predicted. BAIM can estimate not only the energy fluxes but also the carbon dioxide flux between the land surface ecosystem and the atmosphere. The photosynthesis processes for C₃ plants and C₄ plants are adopted in the model.

Off-line verifications of BAIM in a snowless condition were made using the point micrometeorological data observed at a grassland. In general, the fluxes simulated by the model agreed well with those observed (Fig.2). In particular, clear differences between the results using the parameters for C₃ plants and those using the parameters for C₄ plants appeared in the net carbon dioxide fluxes.

To investigate the influence of variations in the values of parameters related to the property of vegetation, sensitivity tests of the model were conducted. By changing the values of the parameters by $\pm 50\%$, the maximum variations of the time-averaged fluxes were obtained. The values of net radiation flux, sensible heat flux, latent heat flux, and soil heat flux were about $\pm 15 \text{ W/m}^2$, $\pm 8 \text{ W/m}^2$, $\pm 9 \text{ W/m}^2$, and $\pm 1 \text{ W/m}^2$, respectively. The maximum variations of the time-averaged value of net carbon dioxide flux were about $\pm 5 \mu \text{ mol/m}^2/\text{s}$ for C₃ parameters and $\pm 7 \mu \text{ mol/m}^2/\text{s}$ for C₄ parameters.

The energy fluxes and carbon dioxide fluxes were also influenced strongly by changes of the soil wetness. As the soil wetness decreased, the net radiation flux, the latent heat flux, and the carbon dioxide accumulation rate decreased, and the sensible heat flux and the respiration rate increased. The accurate estimation of the soil wetness is very important to accurately estimate the energy fluxes and the carbon dioxide flux.

ATMOSPHERIC BOUNDARY LAYER

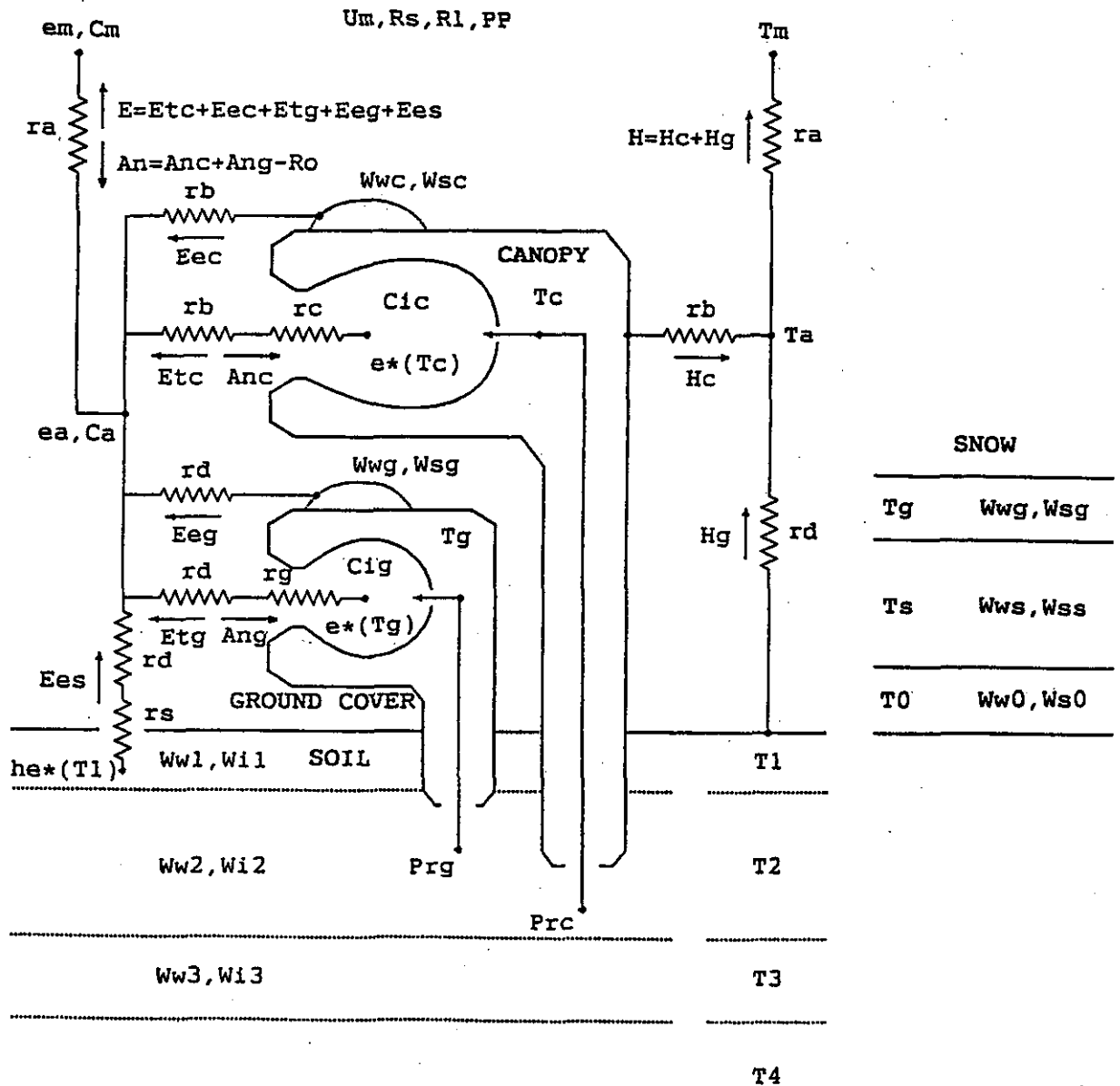


Fig.1 A block diagram of the Biosphere-Atmosphere Interaction Model(BAIM). On the left-hand side, transfer pathways for latent heat flux and carbon dioxide flux are shown. On the right-hand side, the transfer pathways for sensible heat flux are shown.

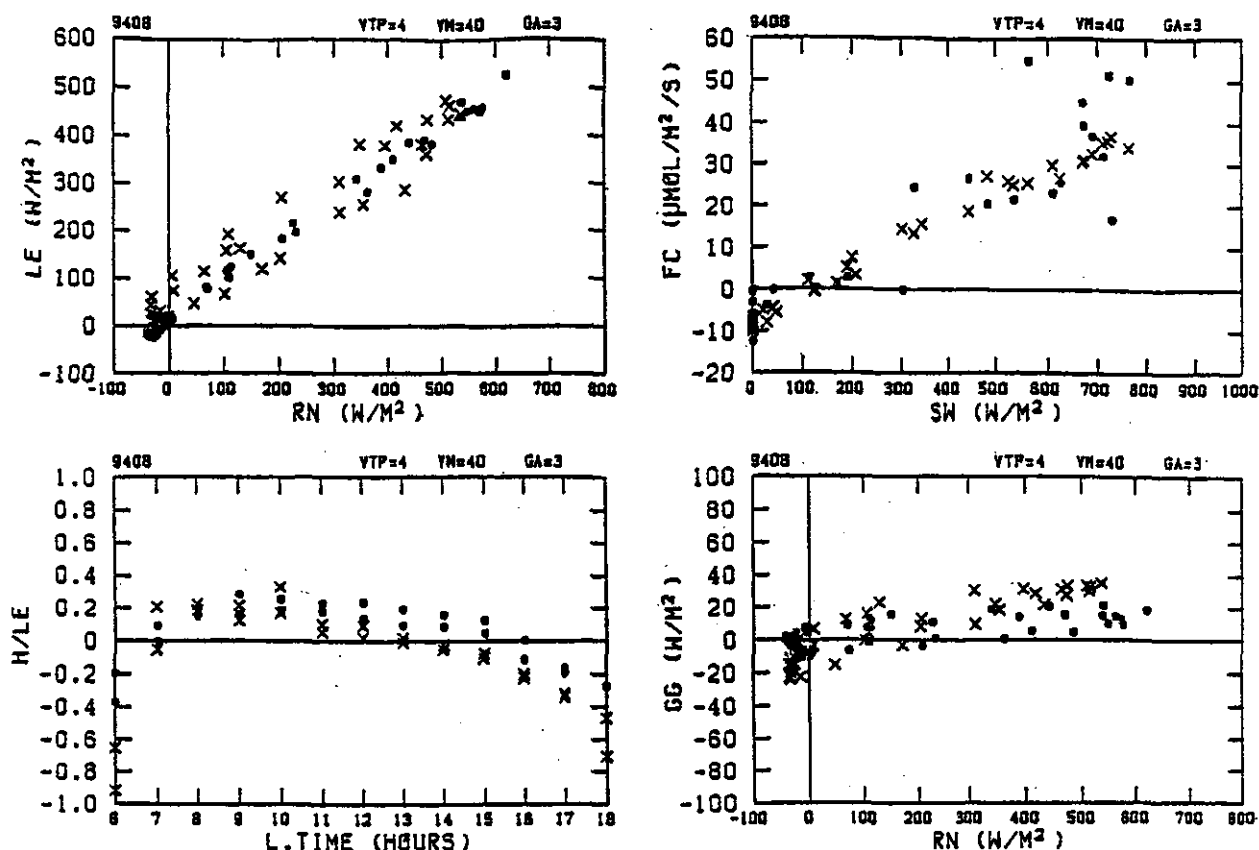


Fig.2 The comparison of observed and calculated fluxes in Aug. Circles are the observations and X symbols are the calculations using the parameters for C_3 plants. LE, latent heat flux (upward flux is positive); RN, net radiation flux (downward flux is positive); H/LE, the Bowen ratio; L.Time, local time; FC, net carbon dioxide flux (downward flux is positive); SW, downward shortwave radiation flux (observed value); GG, heat flux into the soil (downward flux is positive).

3.2 A Model and Observational Study of CO_2 and H_2O Exchange Between Atmosphere and Grassland Ecosystem

On the other hand, the aim of the present study in University of Tsukuba is to measure CO_2 flux by the gradient method over a grassland containing C_3 and C_4 plants. The seasonal change in CO_2 flux measured by the gradient method was analyzed from the ecological and meteorological point of view over an artificial grassland containing C_3 and C_4 plants in University of Tsukuba. The three dominant species of the grassland belonged to the Gramineae; *Festuca elatior* (C_3) dominated in early spring, and *Imperata cylindrica* (C_4) and *Andropogon virginicus* (C_4) grew during early summer and became dominant

in mid-summer (Fig.3).

Data of the surface heat budget were used to analyze the CO_2 and H_2O exchange between the grassland and the atmosphere. From August to October in 1993, CO_2 flux decreased even under the same solar radiation conditions. The monthly values of water use efficiency, i.e., the ratio of CO_2 flux to H_2O flux decreased from 5.2 to 2.9 $mgCO_2/gH_2O$ from August to October, while the Bowen ratio increased from 0.20 to 0.30, and the ratio of the bulk latent heat transfer coefficient CE to the sensible heat transfer coefficient CH was maintained around 0.40 - 0.50 during the same period.

The increase in the Bowen ratio was explained by the decrease in monthly mean air temperature from $22.3^\circ C$ in August to $16.6^\circ C$ in October without considering biological effects such as

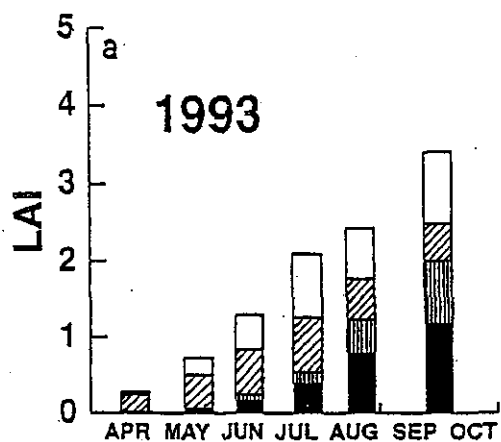


Fig.3 Seasonal variation of leaf area index, a:1993,b:1994.

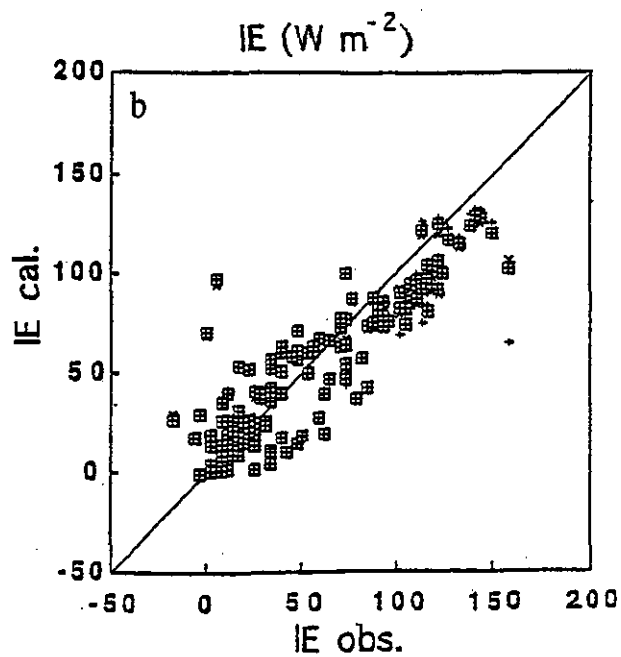
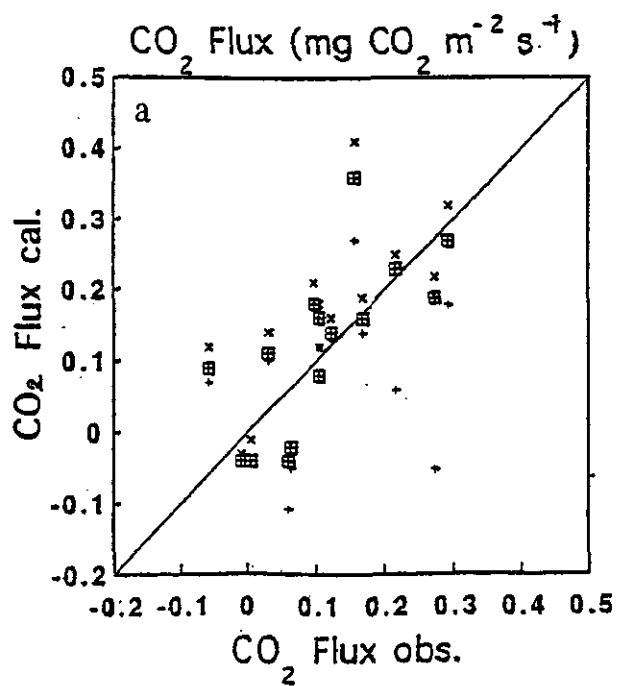
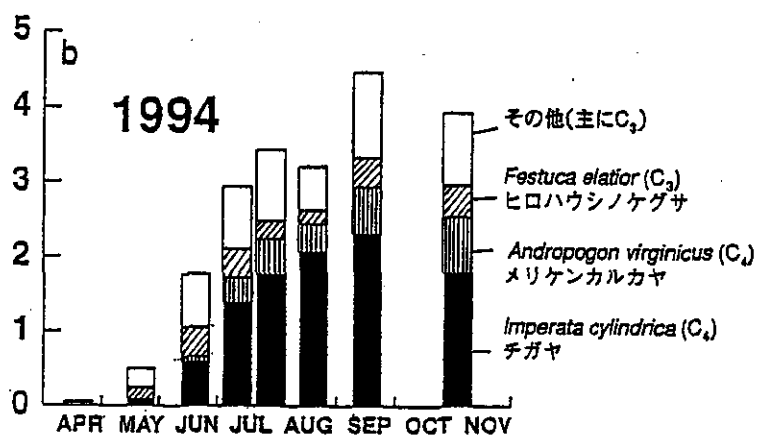


Fig.4 A comparison of computed CO₂ flux (a) and latent heat flux (b) with those observed. +: C₃ plants, ×: C₄ plants, ⊕: C₃, C₄ mixed grasslands.

stomatal closure on the individual leaves. The nearly constant CE/CH ratios suggested that the contribution ratio of canopy resistance to the aerodynamic resistance of the canopy did not change remarkably, although the meteorological conditions changed seasonally. The decrease in the water use efficiency, however, suggested that the photosynthesis rate decreased on the individual leaves from August to October under the same radiation conditions.

Diurnal variations of CO₂ exchange were simulated by the multi-layer canopy model which took the differences in the stomatal conductance and photosynthetic pathway between C₃ and C₄ plants into account. The results suggested that the decrease in the net canopy CO₂ exchange from August to October was induced partly by the relative decrease of the contribution of C₄ plants to the canopy photosynthesis, and also by the decrease of net photosynthesis on the individual leaves in both C₄ and C₃ plants, which could be due to aging of the leaves (Fig. 4). Further studies are required to develop a methodology of observing and predicting the seasonal changes in the characteristics of CO₂ and H₂O fluxes over vegetated surfaces, based on photosynthetic and transpirative processes on the scale of individual leaves.

References

- 1) Dickinson, R.E., Modeling evapotranspiration for three-dimensional global climate models, *Geophys. Monograph*, 29, 58-72, 1984.
- 2) Sellers, P. J., Y. Mintz, Y. C. Sud, and A. Dalcher. A simple biosphere model (SiB) for use within general circulation models, *J. Atmos. Sci.*, 43, 505-531, 1986.
- 3) Dickinson, R.E., and A. Henderson-Sellers. Modelling tropical deforestation: A study of GCM land-surface parameterizations. *Quart. J. R. Meteorol. Soc.*, 114, 439-462, 1988.
- 4) Sato, N., P. J. Sellers, D.A. Randall, E. K. Schneider, J. Shukla, J. L. Kinter III, Y.-T. Hou and E. Albertazzi. Effects of implementing the simple biosphere model in a general circulation model. *J. Atmos. Sci.*, 46, 2757-2782, 1989.
- 5) Horie, T. System ecological studies on crop-weather relationships in photo-synthesis, transpiration and growth, *Bull. Natl. Inst. Agric. Sci.*, 28, 1-181, 1981, (in Japanese with English summary).
- 6) Ohtaki, E. On the similarity in atmospheric fluctuations of carbon dioxide, water vapor and temperature over vegetated fields, *Boundary-Layer Meteorol.*, 32, 25-37, 1985.
- 7) Baldocchi, D. A comparative study of mass and energy exchange rates over a closed C₃ (wheat) and an open C₄ (corn) crop: II. CO₂ exchange and water use efficiency. *Agric. For. Meteorol.*, 67, 291-321, 1994.
- 8) Fan, S.-M., M. L. Goulden, J. W. Munger, B.C. Daube, P. S. Bakwin, S. C. Wofsy, J. S. Amthor, D.R. Fitzjarrald, K.E. Moore, and T.R. Moore. Environmental controls on the photosynthesis and respiration of a boreal lichen woodland: a growing season of whole-ecosystem exchange measurements by eddy correlation. *Oecologia*, 102, 443-452, 1995.
- 9) Oikawa, T. A simulation study of grassland carbon dynamics as influenced by atmospheric CO₂ concentration In: Murai, S. (Ed.), *Toward global planning of sustainable use of the earth*, 97, 112, 1995.
- 10) Hattersley, P.W. The distribution of C₃ and C₄ grasses in Australia in relation to climate. *Oecologia*, 57, 113-128, 1983.
- 11) Cavagnaro J. B. Distribution of C₃ and C₄ grasses at different altitudes in a temperate arid region of Argentina. *Oecologia*, 76, 273-277, 1988.
- 12) Kalapos T. C₃ and C₄ grasses of Hungary: environmental requirements, phenology and role in the vegetation, *Abstracta Botanica*, 15, 83-88, 1991.

Destratification and gravitational circulation causing Aoshio in Tokyo Bay

Contact Person Masataka Watanabe
Division of Water and Soil Environment
National Institute for Environmental Studies

Research Organization Masataka Watanabe NIES
Shigeki Harada NIES
Kunihiko Amano NIES
Yuji Ishikawa NIES

Keywords anoxic water, upwelling, destratification, eutrophication,
gravitational circulation, Aoshio, surface cooling, off-shore wind

1. Introduction

The region of hypoxic bottom water has increased over the past 20 yrs due to eutrophication caused by the increase in the discharge of organic matter as well as nutrients into Tokyo Bay.

Freshwater supply during wet season (early summer) and subsequent hot weather during summer lead to high stability, a condition which persists through late September. Oxygen depletion and the formation of hydrogen sulfide occur in the lower layer during stratified period. The transition from the stably stratified summer regime to the fall destratification was found to occur abruptly when rapid cooling of surface water and strong continuing northerly off-shore wind persisted. In such period coastal upwelling of sulfidic bottom water occurs and the water color becomes milky blue-green, which is called Aoshio.

The Aoshio (milky blue-green water) has been observed in Tokyo Bay since 1950's. The colloidal elemental sulfur and manganese-rich particles identified in the Aoshio water appear to be oxidation products of dissolved sulfide and manganese (II) in the anoxic water which has been observed near the bottom during summer (Takeda et al., 1991). Elemental sulfur existed in the boundary layer between oxygen-sufficient water and anoxic bottom water, indicating that sulfur particles was formed rapidly by vertical mixing at the

boundary layer.

In this analysis the physical mechanism causing Aoshio event in Tokyo Bay was investigated by using the three-dimensional circulation model.

2. Model description

The circulation model used in this investigation was a three dimensional model describes velocities (u , v , w) and salinity (s) developed by Blumberg and Mellor (1983), Blumberg and Goodrich (1990). The second-order turbulence closure scheme of Mellor and Yamada (1982) was used in order to express the variation of vertical mixing due to wind and surface cooling. The temperature model was developed by Watanabe (1994). Horizontal grid size was 1km X 1km and vertical resolution was 10 vertical grid points using a depth-conforming vertical coordinate (sigma system) which was sufficient to resolve surface wind-mixed and bottom tidal mixed boundary layers.

The major sources of freshwater discharges were from the rivers of Tsurumi, Tama, Sumida, Arakawa, Edo and upstream of 10km was included as computational domain. Daily averaged freshwater discharges from these rivers (Table of river flow, Ministry of Construction) were imposed. Tidal forcing was given from harmonic constants obtained at Jogashima and Iwaibukuro tide gauge stations. Daily averaged air temperature, solar

radiation, cloud cover, relative humidity and wind velocity were obtained from Chiba meteorological station. Boundary conditions of temperature and salinity at open ocean were obtained from water quality data-base of Kanagawa Prefecture Fishery Station. Initial conditions of temperature and salinity were obtained from water quality data-base of Environment Agency.

Simulation was conducted from July 1, 1989 to October 21, 1989 and time step of $\Delta t=10$ sec was used.

3. Results

Outbreaks of Aoshio in Tokyo Bay had been reported five times from June to October in 1989 and strong northerly off-shore wind persisted in all cases. Outbreaks in October 2, 1989 was rather large scale and detail measurements of velocity, salinity, temperature were conducted from September 11,

1989 to October 21, 1989 at 4 points in Tokyo Bay (Oshima et al., 1989). Simulated temperature and salinity were compared with observed data (Fig. 1, 2; measured at st. A; $35^{\circ} 34'00''N$, $139^{\circ} 58'30''E$) and in general excellent agreements were obtained. In September 28, strong south-wind blew and vertical wind mixing increased but it did not persisted (Table 1). Air temperatures were always higher than water temperatures until September 28, and surface cooling did not occur (Table 1). In September 29, north-wind started to blow and continued until October 15. Air temperature became lower than water temperature from October 1, and vertical eddy diffusivity increased between October 2 and October 4 due to the coupling effects of surface wind mixing and surface cooling, which promoted abrupt destratification. Off shore wind driven current coupled with increased vertical eddy diffusivity created strong up-welling near the coast between

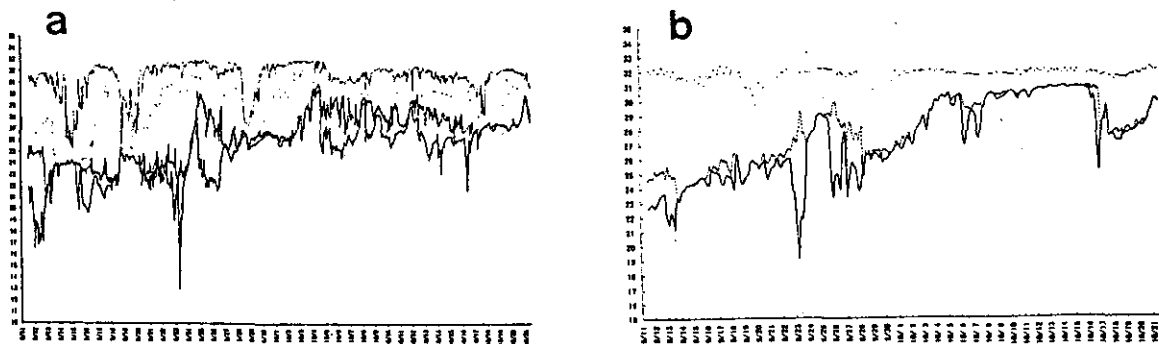


Fig. 1 Time series of salinity at station A. (a) observed (b) predicted.

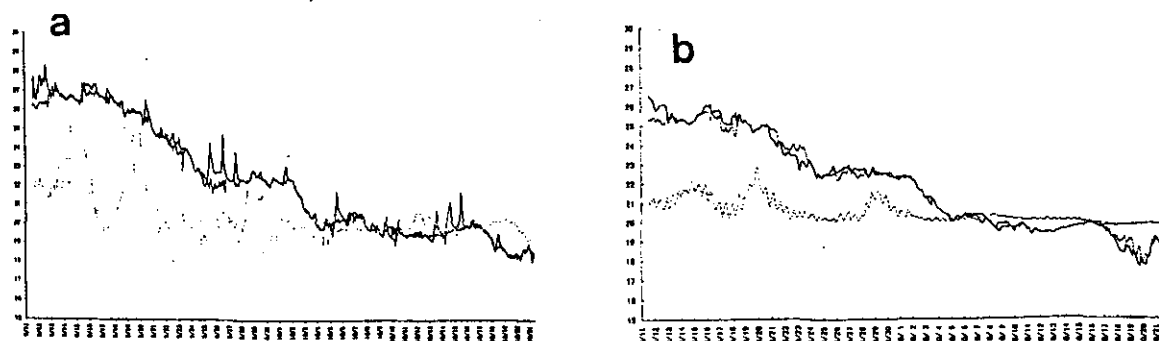


Fig. 2 Time series of temperature at station A. (a) observed (b) predicted.

Funabashi Harbor and Chiba Harbor (Fig. 3), which formed gravitational circulation in entire Bay scale (Fig. 4).

Physical conditions for the outbreaks of Aoshio were abrupt destratification due to wind mixing and surface cooling and strong up-welling due to gravitational circulation.

	T air	T water	K _H
9/26	22.8	21.6	10X10 ⁻⁵ (m2s ⁻¹)
27	26.0	21.8	16
28	23.0	22.0	192
29	20.8	21.8	7
30	21.9	21.4	2
10/1	19.2	21.2	1
2	18.8	20.4	27
3	17.9	19.8	57
4	20.2	19.5	24
5	19.9	19.4	5

Table 1 Calculated vertical eddy diffusivity during the outbreaks of Aoshio in 1989

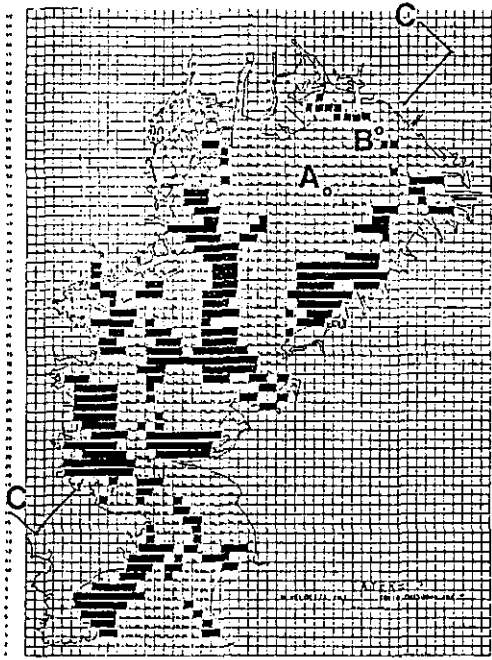


Fig 3 Horizontal distribution of vertical velocities
(white : up welling, dark : down welling)
A : location of station A, B : location of the point where vertical eddy diffusivity was calculated, c-c : vertical cross section.

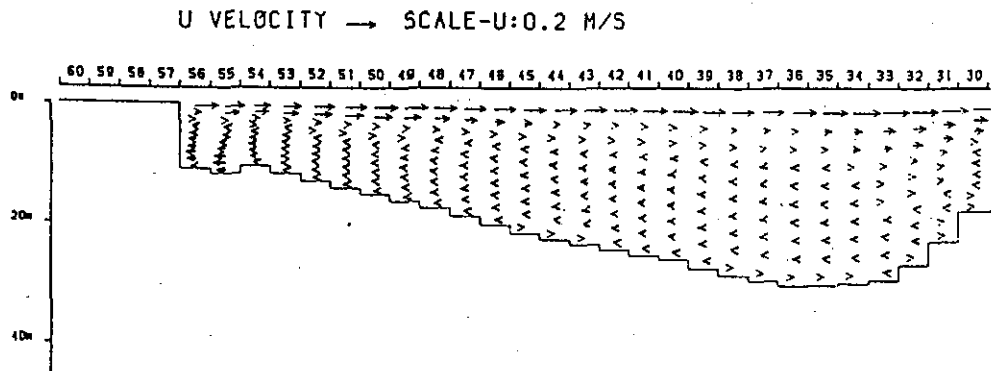


Fig. 4 Velocity distribution across the section c-c shown in Fig. 3.

References

Blumberg, A. F. and Goodrich, D. M. 1990. Estuaries. 13, 236-249.

Blumberg, A. F. and Mellor, G. L. 1983. J. Giophys, Res. 88, 4479-4592.

Mellor, G. L. and Yamada, T. 1982. Review of Geophysics and Space Physics. 20, 851-875.

Oshima, S., Odamaki, M., Shimohira, Y.,

Matsushima, H., Nishida, H. and Sato, S. 1989. Environment Agency Research Report in 1989. P.103-II-1-103-II-12.

Takeda, S., Nimura, Y. and Hirano, R. 1991. J. Oceanogr. Society of Japan. 47, 126-137.

Watanabe, M. 1992. CGER'S Super Computer Activity Report 1992, vol.1. 46-49.